SPANDIDOS PUBLICATIONS

ONCOLOGY REPORTS 49: 60, 2023

LAPTM5 regulated by FOXP3 promotes the malignant phenotypes of breast cancer through activating the Wnt/β-catenin pathway

SIJIA HAN, XUEYING JIN, TIANYU HU and FENG CHI

Department of Oncology, Shengjing Hospital of China Medical University, Shenyang, Liaoning 110022, P.R. China

Received June 21, 2022; Accepted December 22, 2022

DOI: 10.3892/or.2023.8497

Abstract. Breast cancer remains the most common malignancy and the leading cause of cancer-associated mortality in women worldwide. Lysosomal protein transmembrane 5 (LAPTM5), a lysosomal membrane protein, plays an important role in several human malignancies. However, the biological functions and mechanism of LAPTM5 in breast cancer remain unclear. In the present study, the potential tumor-promoting effect of LAPTM5 was predicted by bioinformatics analysis. LAPTM5 was highly expressed in breast cancer clinical specimens. Moreover, *in vitro* studies demonstrated that cell proliferation, migration and invasion, as well as the process of epithelial-mesenchymal transition (EMT) were promoted by LAPTM5 overexpression and were suppressed by LAPTM5 downregulation *in vitro*. The tumor-promoting effects of LAPTM5 were also confirmed by xenograft tumor assay *in vivo*. It was found that the tumor-promoting effects of LAPTM5 were partly dependent on the activation of the Wnt/β-catenin signaling pathway. Furthermore, dual-luciferase and chromatin immunoprecipitation assays verified that the transcription factor forkhead box protein 3 (FOXP3) directly bound to the promoter of LAPTM5 and negatively regulated its expression. Taken together, the present findings indicated that LAPTM5, negatively regulated by FOXP3, promoted the malignant phenotypes of breast cancer through activating the Wnt/β-catenin signaling pathway.

Introduction

Breast cancer is the most frequent malignant tumor and the leading cause of high mortality induced by cancer in women worldwide (1,2). In 2009, it was reported that this disease affects 10-12% of the female population each year and causes half a million deaths worldwide (3). Despite recent advances in diagnosis and treatment, tumor invasiveness and cell migration capability remain the crucial factors affecting patient survival (4-6). Epithelial-mesenchymal transition (EMT) is the process by which epithelial cells lose cell adhesion, enhance tumor migration and cell invasion ability, and acquire mesenchymal characteristics (7,8). It is associated with basal-like breast tumors, producing cells with stem-like properties, and allowing cancer cells to spread and metastasize (9). Reducing the metastasis and invasion ability of breast cancer cells is crucial to improve the prognosis and reduce the mortality of patients with breast cancer. However, the molecular mechanism of cell migration and invasion in breast cancer remains to be further explored.

Lysosomal protein transmembrane 5 (LAPTM5), also known as CD40-ligand-activated specific transcript 6 (CLAST6), is a lysosomal membrane protein that has been identified as a key role in the diagnosis and prognosis of human cancer (10). For testicular germ cell tumor (TGCT), LAPTM5 was identified as a potential biomarker (11). Chen *et al* (12) demonstrated that LAPTM5 was highly expressed in bladder cancer tissue, and the decrease in LAPTM5 suppressed the proliferation and viability of bladder cancer cells. Moreover, LAPTM5 was found to be closely associated with poor prognosis of patients with clear cell renal cell carcinoma (CCRCC) and was identified as a potential therapeutic target (13). Additionally, LAPTM5 expression was analyzed by using the Genotype-Tissue Expression (GTEx) and The Cancer Genome Atlas (TCGA) datasets, and it was found that LAPTM5 was upregulated in breast tumor tissues. Therefore, it was hypothesized that LAPTM5 may be a potential molecular therapeutic target to improve the accuracy of breast cancer diagnosis. Thus, the role of LAPTM5 in breast cancer needs to be explored.

Forkhead box protein 3 (FOXP3) is a member of the FOX protein family (14), which participates in the regulation of the occurrence and development of various human tumors (15). It has been reported that FOXP3 inhibits tumorigenesis and metastasis through binding to the promoter of certain genes (16-18). FOXP3, as a transcription factor necessary to regulate the differentiation and function of T cells, affects the development and function of T cells, thereby affecting the proliferation of tumors. Ladoire *et al* (19) revealed that breast cancer patients with high FOXP3 expression have a

Correspondence to: Dr Feng Chi, Department of Oncology, Shengjing Hospital of China Medical University, 39 Huaxiang Road, Shenyang, Liaoning 110022, P.R. China
E-mail: chifeng7109@163.com and chif@sj-hospital.org

Key words: breast cancer, lysosomal protein transmembrane 5, forkhead box protein 3, Wnt/β-catenin pathway, epithelial-mesenchymal transition

lower tumor grade and a better prognosis. However, studies on FOXP3 in breast cancer cells are limited. According to database predictions, FOXP3 is expected to bind the LAPTM5 promoter. The present study aimed to explore the association between FOXP3 and LAPTM5, and the mechanism by which LAPTM5 may affect breast cancer.

The Wnt/β-catenin signaling pathway is ubiquitous in organisms, and it is an important signaling pathway that regulates cell proliferation and differentiation (20,21). It participates in the tumor microenvironment and contributes to the initiation and progression of various human cancer types (22-24). β-catenin is a key factor of the Wnt signaling pathway, that could promote the transcription of target genes regulated by Wnt/β-catenin (25). In breast cancer, Wnt/β-catenin is the main signaling pathway that induces the EMT of cancer cells, and has been identified as an important mediator of cell metastasis and a marker of poor prognosis (9,26). Therefore, it is necessary to verify whether this signaling pathway mediates the effect of LAPTM5 on breast cancer.

In the present study, bioinformatic analysis was used to predict the potential function of LAPTM5 on breast cancer. LAPTM5 was found to be overexpressed in clinical specimens of patients with breast cancer. *In vitro* experiments verified that LAPTM5 could promote breast cancer cell proliferation, migration and invasion as well as EMT through positive regulation of β-catenin. Moreover, LAPTM5 was demonstrated to promote tumor malignant phenotypes *in vivo*, and it was suppressed by transcriptional regulation of FOXP3. Taken together, the present findings revealed the function and molecular mechanism of LAPTM5 in breast cancer.

Materials and methods

Bioinformatics analysis. The expression of LAPTM5 in breast cancer tissues and the association between LAPTM5 and various clinical indicators were analyzed using Breast Cancer Gene-Expression Miner (bcGenExMiner v4.8; http://bcgenex.centregauducheau.fr/BC-GEM) (27). The association between patient overall survival and LAPTM5 was evaluated with the Kaplan-Meier plotter (http://kmplot.com/analysis/index.php?p=background) (28). The log-rank test was performed at the same time.

Tissue collection. The breast cancer samples and para-carcinoma tissues were obtained from 40 patients (24-82 years old) who had been diagnosed at the Shengjing Hospital of China Medical University from March to May in 2019. The samples were collected by biopsy and stored at -80˚C until total RNA was extracted. The collection and analysis of patient samples were approved (approval no. 2019PS339K) by the ethics committee of Shengjing Hospital of China Medical University (Shenyang, China). Written informed consent was provided by all patients.

Cell culture and transfection. Human normal breast epithelial cells (MCF-10A) and breast cancer cell lines (MDA-MB-453, MDA-MB-231 and MCF-7) were purchased from iCell Bioscience Inc., while the breast cancer cell lines SK-BR-3 and T-47D were purchased from Procell Life Science and Technology Co., Ltd. All cell lines were cultured at 37˚C in a 5% CO_2 incubator. The MCF-10A cell line was cultured in its specific medium (iCell Bioscience Inc.), while MDA-MB-453 and MDA-MB-231 cells were cultured in L-15 medium (Procell Life Science and Technology Co., Ltd.) with 10% fetal bovine serum (FBS) (Zhejiang Tianhang Biotechnology Co., Ltd.). SK-BR-3 cells were cultured in McCoy's 5A medium (Procell Life Science and Technology Co., Ltd.) containing 10% FBS. T-47D cells were cultured in RPMI-1640 medium (Beijing Solarbio Science and Technology Co., Ltd.), while MCF-7 cells were cultured in MEM (Beijing Solarbio Science and Technology Co., Ltd.), both containing 10% FBS. MDA-MB-231 and T-47D cells were confirmed to be free from mycoplasma and were verified by STR profiling.

Cells ($4x10^5$ cells per well) were dispensed into six-well plates and incubated in an incubator at 37˚C. After the confluency of cells reached 60%, T-47D cells were transfected with 2.5 μg OE-Vector (pcDNA3.1, Chongqing Unibio Biological Technology Co., Ltd.) or OE-LAPTM5, and MDA-MB-231 cells were transfected with 2.5 μg sh-NC (5'-TTCTCCGAA CGTGTCACGT-3'), sh-LAPTM5-1 (sh-1: 5'-GGTGCTACA GATTGATCAA-3') or sh-LAPTM5-2 (sh-2: 5'-GCGTCTTGT TGTTCATCGA-3') using Lipofectamine™ 3000 (Invitrogen; Thermo Fisher Scientific, Inc.). After 48 h, MDA-MB-231 medium was changed to complete medium containing 400 μg/ml G418 (Shanghai Aladdin Biochemical Technology Co., Ltd.), and T-47D medium was replaced with complete medium containing 450 μg/ml G418. Medium of the two cell lines was changed every 2 days. After one week, the medium was changed to complete medium and cultured for almost 10 days. Multiple monoclonal cell clusters in the medium were continued to subculture to obtain stably transfected cell lines.

Reverse transcription-quantitative PCR (RT-qPCR). Total RNA was extracted from cells with TRIpure reagent (BioTeke Corporation), and cDNA was synthesized using a kit named Super M-MLV reverse transcriptase (BioTeke Corporation) and RNase inhibitor (BioTeke Corporation) according to the manufacturer's instructions. Next, cDNA was mixed with SYBR Green (Sigma-Aldrich; Merck KGaA), primers, and 2X Power Taq PCR Master Mix (BioTeke Corporation), and the mixture was subjected to RT-qPCR in an Exicycler™ 96 Real-Time Quantitative Thermal Block (Bioneer Corporation) according to the manufacturer's instructions. The mRNA expression levels of the target genes were calculated via the $2^{-\Delta\Delta Cq}$ method (29) using β-actin as the control. The primers were synthesized by GenScript and the sequences were as follows: LAPTM5 forward, 5'-AGCGTCTTGTTGTTC ATCG-3' and reverse, 5'-GCAGGCACAGGAGATAGTC-3'; β-catenin forward, 5'-CAAGTGGGTGGTATAGAGG-3' and reverse, 5'-GGATGGTGGGTGTAAGAG-3'; FOXP3 forward, 5'-TGACCAAGGCTTCATCTGTG-3' and reverse, 5'-GAG GAACTCTGGGAATGTGC-3'; and β-actin forward, 5'-GGC ACCCAGCACAATGAA-3' and reverse, 5'-TAGAAGCAT TTGCGGTGG-3'. The thermocycling conditions were as follows: 94˚C for 5 min; 40 cycles of 15 sec at 94˚C, 25 sec at 60˚C, 30 sec at 72˚C; 72˚C for 5.5 min; 40˚C for 2.5 min; 60˚C to 94˚C, 1.0˚C/1 sec; 25˚C for 1-2 min.

Western blotting. Whole protein extracts were prepared using cell lysis buffer (Beyotime Institute of Biotechnology)

with phenylmethanesulfonylfluoride (Beyotime Institute of Biotechnology) at a final concentration of 1 mM. The BCA Protein Assay kit (cat. no. P0011; Beyotime Institute of Biotechnology) was used to detect the concentration of total proteins according to the manufacturer's instructions. Total proteins were separated by SDS-PAGE and electro-transferred onto polyvinylidene fluoride membranes (MilliporeSigma). The concentration of stacking gel was 5%. Different concentrations of separating gel were used to detect different proteins. Proteins, including LAPTM5, FOXP3, CyclinD1, CyclinA, CDK2, CDK4, MMP2, MMP9 and β-actin, were detected under the 12% separating gel. E-cadherin, N-cadherin and β-catenin were examined using 8% separating gel. Histone H3 was evaluated in 14% separating gel. After being blocked with 5% non-fat milk for 1 h at room temperature, the membranes were probed with primary antibodies overnight at 4˚C. β-actin was used as a loading control, and its loaded amount was consistent with the detected proteins. Next, membranes were incubated with HRP-conjugated IgG antibodies for 45 min at 37˚C. The secondary antibodies were incubated with proteins loaded at the aforementioned amount after treatment with primary antibodies. Therefore, protein loaded amount of secondary antibodies was also consistent with the detected proteins. Enhanced chemiluminescence (ECL) (Beyotime Institute of Biotechnology) was used to visualize the immunoreactive proteins. Details of the aforementioned antibodies are listed in Table SI.

Cell counting kit-8 (CCK-8) assay. Stably transfected cells were plated into 96-well plates ($3x10^3$ cells per well). After cell culture for 0, 24, 48, 72 and 96 h, 10 μl CCK-8 solution (Beyotime Institute of Biotechnology) was added to each well, and the cells were incubated for 2 h at 37˚C. When exploring the effect of β-catenin on LAPTM5-induced cell proliferation, CCK-8 solution was added to the wells after cell culture for 48 h. The absorbance of the plate at 450 nm was measured with a microplate reader (BioTek Instruments, Inc.).

Flow cytometric analysis. Cells were cultured in 6-well plates until they reached 90%. A total of $5x10^5$ cells was collected, and 70% pre-cooled ethanol was added and fixed for 12 h at 4˚C. The samples were processed with a Cell Cycle Analysis kit (cat. no. C1052; Beyotime Institute of Biotechnology) according to the manufacturer's instructions. Next, a flow cytometer (ACEA Biosciences Inc.) was used to detect the cell cycle. The software used for flow cytometric analysis was NovoExpress (version: 1.4.1; Agilent Technologies Inc.).

Wound healing assay. Cells ($4x10^5$ cells per well) were seeded in six-well plates. When cells reached 100%, medium was then changed to serum-free medium containing 1 μg/ml mitomycin C (Sigma-Aldrich; Merck KGaA) for 1-h treatment. Next, a sterile 200-μl pipette tip was used to create a straight wound. The same location on each well was recorded with a microscope (magnification, x100) (Olympus Corporation). The cell migration distance was calculated after 24 h. The migration ratio was calculated using the following formula: Migration rate=(0 h width of wound -24 h width of wound)/0 h width of wound x100%.

Transwell assay. Transwell chamber was placed in a 24-well plate and coated with 40 μl diluted Matrigel (Corning, Inc.), which was solidified in an incubator at 37˚C for 2 h. Cells were collected and diluted to form a cell suspension. A total of 200 μl this cell suspension ($1.5x10^4$ cells per well) was added to the upper chamber containing Matrigel. The pore size of the Transwell chamber inserts was 8.0 μm. In the lower chamber, 800 μl medium containing 10% FBS was added as a chemoattractant. After cell culture for 24 h, 4% paraformaldehyde was used to fix the cells for 20 min at room temperature. Next, the cells were stained with 0.5% crystal violet for 5 min. An inverted microscope (magnification, x200) was used to observe invasive cells into the lower chamber. Each sample was randomly selected 5 fields of view to count the number of cells.

Immunofluorescence (IF) analysis. Cells ($8x10^4$ cells per well) were planted in 24-well plates. When cells reached 70%, they were fixed in 4% paraformaldehyde for 15 min at room temperature and incubated in 0.1% Triton X-100 for 30 min at room temperature. After blocking with 1% bovine serum albumin (cat. no. A602440-0050; Sangon Biotech Co., Ltd.) for 15 min at room temperature, the cells were incubated with a β-catenin antibody (1:200; cat. no. ab32572; Abcam) overnight at 4˚C. The bound antibody was visualized using an Alexa Fluor™ 555-labeled goat anti-rabbit IgG antibody (1:200; cat. no. A27039; Invitrogen; Thermo Fisher Scientific, Inc.). Then, the cell nuclei were counterstained with 5 μg/ml 4'-6-diamidino-2-phenylindole (cat. no. D106471-5 mg; Shanghai Aladdin Biochemical Technology Co., Ltd.) for 5 min at room temperature. Images were captured using a fluorescence microscope (magnification, x400).

Xenograft mouse model. To evaluate tumorigenicity *in vivo*, a total of 24 6-week-old BALB/c female nude mice (18±1 g) were divided into 4 groups (n=6 per group). The mice could eat and drink freely, and were raised in an environment of temperature 22±1˚C, humidity 45-55%, and 12 h light/dark cycle every day. Cells transfected with different vectors were collected and prepared into cell resuspension solution respectively. Cells ($1x10^7$) were subcutaneously injected into the dorsal side of the right armpit of these mice. The tumor volume was measured every 3 days and was calculated by the following formula: Volume=1/2 x length x width^2. At the end of the experiment, mice were treated by 5% isoflurane for induction of anesthesia followed by performing cervical dislocation. Tumors were removed and images were captured. A portion of the tumor tissue was fixed with 4% paraformaldehyde at room temperature for more than 24-48 h for subsequent experiments. All experiments involving animals were approved (approval no. 2019PS339K) by the animal ethics committee of Shengjing Hospital of China Medical University (Shenyang, China).

Immunohistochemistry (IHC). Tumor tissue sections were prepared and subjected to IHC analysis. Anti-KI67 antibody (1:100; cat. no. 27309-1-AP; ProteinTech Group, Inc.) and anti-LAPTM5 (1:100; cat. no. bs-17100R; BIOSS) antibody were used as primary antibodies, which were added to cover the tissue sections at 4˚C overnight. HRP-conjugated goat anti-rabbit IgG (1:200; cat. no. 31460; Thermo Fisher Scientific,

Inc.) was used as a secondary antibody, which was incubated with tissue sections at 37˚C for 60 min. Next, the sections were treated with a 3,3'-diaminobenzidine (DAB) substrate kit (cat. no. DA1010; Beijing Solarbio Science and Technology Co., Ltd.) and stained with hematoxylin (cat. no. H8070; Beijing Solarbio Science and Technology Co., Ltd.) according to the manufacturer's instructions. The stained results were observed and images were captured under a fluorescence microscope (magnification, x400) (Olympus Corporation).

Dual-luciferase reporter assay. Breast cancer MDA-MB-231 cells ($8x10^4$ cells per well) were seeded in 24-well plates. After cells reached 70%, the cells were co-transfected with pGL3-basic (General Biosystems Co., Ltd.) or pGL3-LAPTM5 promoter sequence and pcDNA3.1 (Chongqing Unibio Biological Technology Co., Ltd.) or pcDNA3.1-FOXP3. A *Renilla* luciferase plasmid was transfected together with a constructed plasmid for normalizing the efficiency of transfection. After 48 h, the luciferase activity was measured with a Dual-Luciferase Reporter Gene Assay kit (Nanjing KeyGen Biotech Co., Ltd.).

Chromatin immunoprecipitation (ChIP) assay. A ChIP assay was performed with a Cell ChIP kit (Wanleibio Co., Ltd.) according to the manufacturer's instructions. Briefly, MDA-MB-231 cells were fixed in 1% paraformaldehyde at room temperature for 10 min and sonicated. Next, the cell lysates were incubated with anti-FOXP3 antibody (undiluted, cat. no. PA1-806; Thermo Fisher Scientific, Inc.) or negative control IgG (undiluted) at 4˚C overnight, then mixed with 60 μl protein A beads at 4˚C. The immunoprecipitated complex was washed from beads through centrifuging at 625 x g for 1 min at 4˚C and the supernatant was collected. The target DNA fragments were then amplified by polymerase chain reaction (PCR), analyzed by 2% agarose gel electrophoresis and visualized using Gold View nuclear staining dye. The PCR reaction system contained 2 μl immunoprecipitated DNAs, 1 μl forward primers, 1 μl reverse primers, and 10 μl 2X Taq PCR Master-mix (BioTeke Corporation), as well as sterile ultra-pure water to adjust total volume to 20 μl. The primer sequences were listed in Table SII. The PCR amplifications were performed under the following conditions: 95˚C for 5 min; 40 cycles of 20 sec at 95˚C, 20 sec at 50˚C, 30 sec at 72˚C; 25˚C for 5 min.

Statistical analysis. Statistical analysis was performed using Prism 7 software (GraphPad Software, Inc.). According to the bc-GenExMiner online tool, differences among the groups of Fig. 1A were analyzed using ANOVA followed by Dunnett-Tukey-Kramer's test. Difference of LAPTM5 mRNA expression between tumor tissues and para-tumor tissues in Fig. 1B was assessed by paired Student's t-test. The results of tumor volume in *in vivo* experiments (Fig. 5A and B) were analyzed by unpaired Student's t-test. Difference among more than two groups was examined by one-way analysis of variance (ANOVA) followed by the Tukey's multiple comparisons test. All data are presented as the mean ± SD. The *in vitro* experiments were performed at least in triplicate, and the *in vivo* experiments were performed in six replicates. P<0.05 was considered to indicate a statistically significant difference.

Results

High LAPTM5 level is associated with poor prognosis of patients with breast cancer. To determine whether LAPTM5 regulates the development of breast cancer, LAPTM5 expression in the GTEx and TCGA datasets was analyzed using the bc-GenExMiner online tool. LAPTM5 mRNA expression in tumor tissue was significantly higher than that in adjacent tissue and healthy tissue (Fig. 1A). LAPTM5 mRNA expression was examined in 40 pairs of breast cancer and para-carcinoma tissue samples, and it was found to be significantly overexpressed in the breast cancer cases (tumor vs. para-tumor, 0.0120±0.0030 vs. 0.0096±0.0023, P<0.01, Fig. 1B).

Next, the association between LAPTM5 and clinical indicators was estimated by bc-GenExMiner. The Scarff-Bloom-Richardson (SBR) grading as a histological grade is useful for the clinical diagnosis and prognosis of breast cancer (30). Breast cancer patients with higher SBR grade were found to express higher LAPTM5 mRNA levels (Fig. 1C). Patients with increased levels of LAPTM5 exhibited a worse Nottingham prognostic index (NPI) (Fig. 1D). Additionally, LAPTM5 was highly expressed in the infiltrating ductal carcinoma and lowly expressed in micropapillary carcinoma (Fig. 1E). Furthermore, LAPTM5 expression was positively associated with human epidermal growth factor receptor-2 status, and negatively associated with estrogen receptor (ER) and progesterone receptor (PR) status (Fig. 1F-H). Moreover, patients with positive nodal status (N^+) displayed increased levels of LAPTM5 (Fig. 1I). Furthermore, LAPTM5 expression in patients with mutated P53 was significantly upregulated compared with that of patients with wild type P53, indicating that LAPTM5 possibly enhanced the development of breast cancer (Fig. 1J). Patients with high expression of KI67 tended to express higher LAPTM5 (Fig. 1K). Survival analysis confirmed that the increase in LAPTM5 was significantly associated with shorter overall survival in patients with breast cancer (Fig. 1L). In summary, these data revealed that LAPTM5 possibly promoted the progression of breast cancer.

LAPTM5 promotes breast cancer cell proliferation. To further investigate the role of LAPTM5 in breast cancer, the protein expression of LAPTM5 was examined in five breast cancer cell lines and one normal breast epithelial cell line by western blotting (Fig. S1A). LAPTM5 mRNA expression was successfully upregulated in the T-47D cell line (Vector vs. LAPTM5, 1.0240±0.1160 vs. 7.2330±0.7315, P<0.01) and was inhibited in the MDA-MB-231 cell line (sh-NC vs. sh-1 vs. sh-2, 0.9489±0.1413 vs. 0.1996±0.0321 vs. 0.2653±0.0311, P<0.01), which was consistent with the changes of protein expression in the two cell lines (Fig. S1B and C). The results of CCK-8 assay demonstrated that the cell viability of T-47D cells was significantly enhanced by LAPTM5 overexpression (Fig. 2A). The optical density (OD) of LAPTM5 overexpression group was higher than that of vector group at 48 h (LAPTM5 vs. vector, 0.942±0.117 vs. 0.654±0.071, P<0.01), 72 h (LAPTM5 vs. vector, 1.173±0.178 vs. 0.879±0.094, P<0.01) and 96 h (LAPTM5 vs. vector, 1.334±0.215 vs. 0.962±0.090, P<0.01). In the MDA-MB-231 cells, the OD level was significantly decreased at 48 h (sh-NC vs. sh-1 vs. sh-2, 0.779±0.091 vs.

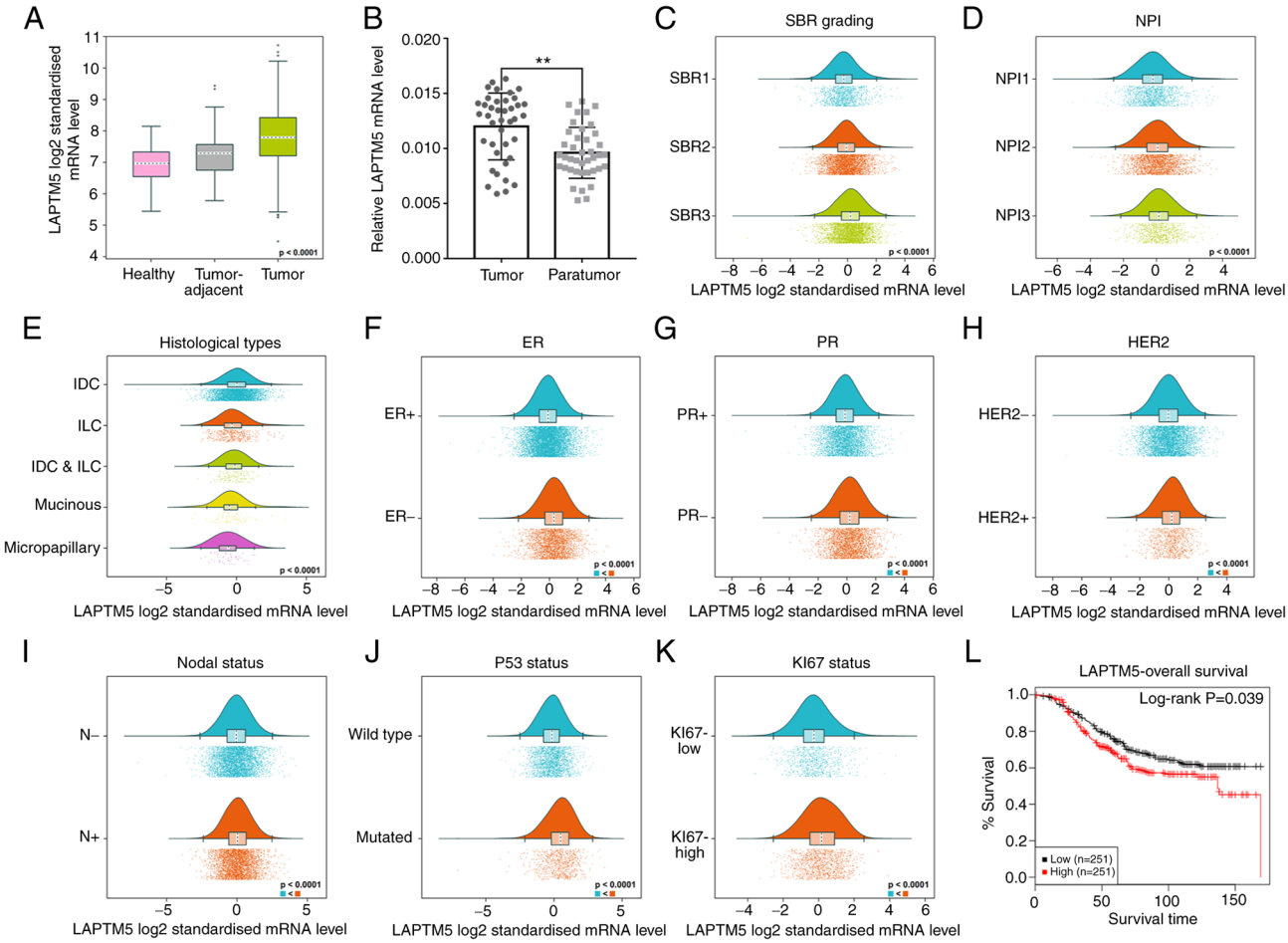

Figure 1. Overexpression of LAPTM5 is associated with a poor outcome of breast cancer. (A) LAPTM5 mRNA level in healthy tissue, tumor-adjacent tissue and tumor was detected by bc-GenExMiner. (B) Reverse transcription-quantitative PCR was used to examine the mRNA expression level of LAPTM5 on breast cancer tissues (n=40) and para-tumor tissues (n=40). Data are presented as the mean ± SD. (C-K) Raincloud plot indicating the association between LAPTM5 and clinical parameters. (L) The relationship between LAPTM5 and overall survival of patients with breast cancer. **P<0.01. LAPTM5, lysosomal protein transmembrane 5.

0.480±0.057 vs. 0.534±0.083, P<0.01), 72 h (sh-NC vs. sh-1 vs. sh-2, 0.854±0.110 vs. 0.618±0.063 vs. 0.587±0.083, P<0.01), and 96 h (sh-NC vs. sh-1 vs. sh-2, 1.015±0.097 vs. 0.627±0.061 vs. 0.661±0.066, P<0.01), indicating cell viability was remarkably suppressed by silencing LAPTM5 (Fig. 2B).

The flow cytometric results showed that the percentage of cells in the G1 phase was reduced (Vector vs. LAPTM5, 61.8±4.1 vs. 43.7±6.9, P<0.01) and increased in the S phase (Vector vs. LAPTM5, 18.1±1.9 vs. 31.2±3.5, P<0.01) by overexpression of LAPTM5 (Fig. 2C). Meanwhile, when LAPTM5 was silenced, cells in G1 phase were upregulated (sh-NC vs. sh-1 vs. sh-2, 63.0±4.6 vs. 75.7±3.2 vs. 77.8±3.4, P<0.01) and them in S phase were decreased (sh-NC vs. sh-1 vs. sh-2, 16.9±1.8 vs. 6.7±0.9 vs. 6.0±0.9, P<0.01, Fig. 2D). Further, the western blot results showed that LAPTM5 overexpression increased the expression of CyclinD1, CyclinA, cyclin-dependent kinase (CDK) 2 and CDK4 in breast cancer cells, while silencing LAPTM5 resulted in the opposite effects (Fig. 2E and F). The aforementioned results indicated that LAPTM5 may be a tumor promoter in breast cancer.

LAPTM5 promotes breast cancer cell migration, invasion and EMT. To further confirm the effects of LAPTM5 on breast cancer metastasis and invasiveness, wound-healing, Transwell and western blot assays were performed. The relative cell migration ratio was significantly increased by LAPTM5 overexpression (Vector vs. LAPTM5, 51.1±7.1 vs. 80.4±6.9, P<0.01, Fig. 3A), and was suppressed by sh-1 (sh-NC vs. sh-1, 63.6±8.5 vs. 40.6±5.2, P<0.05) or sh-2 (sh-NC vs. sh-2, 63.6±8.5 vs. 38.1±5.4, P<0.01, Fig. 3B). In addition, the number of invasive cells was significantly increased when LAPTM5 was overexpressed (Vector vs. LAPTM5, 104.7±12.3 vs. 253.2±45.5, P<0.01, Fig. 3C), while opposite trends were observed after downregulation of LAPTM5 (sh-NC vs. sh-1 vs. sh-2, 107.5±12.8 vs. 55.9±4.9 vs. 59.7±7.9, P<0.01, Fig. 3D). The western blot results showed that the expression of matrix metallopeptidase (MMP) 2 and MMP9 was upregulated with overexpression of LAPTM5, and downregulated with depleting LAPTM5 (Fig. 3E). When LAPTM5 was overexpressed, the expression of E-cadherin was reduced, while N-cadherin was upregulated. When LAPTM5 was silenced, the opposite effects were observed (Fig. 3F). Previous studies reported that E-cadherin was a tumor suppressor that functioned as an inhibitor of cell metastasis (31), while N-cadherin could induce or enhance the metastatic capacity of invading carcinoma cells (32).

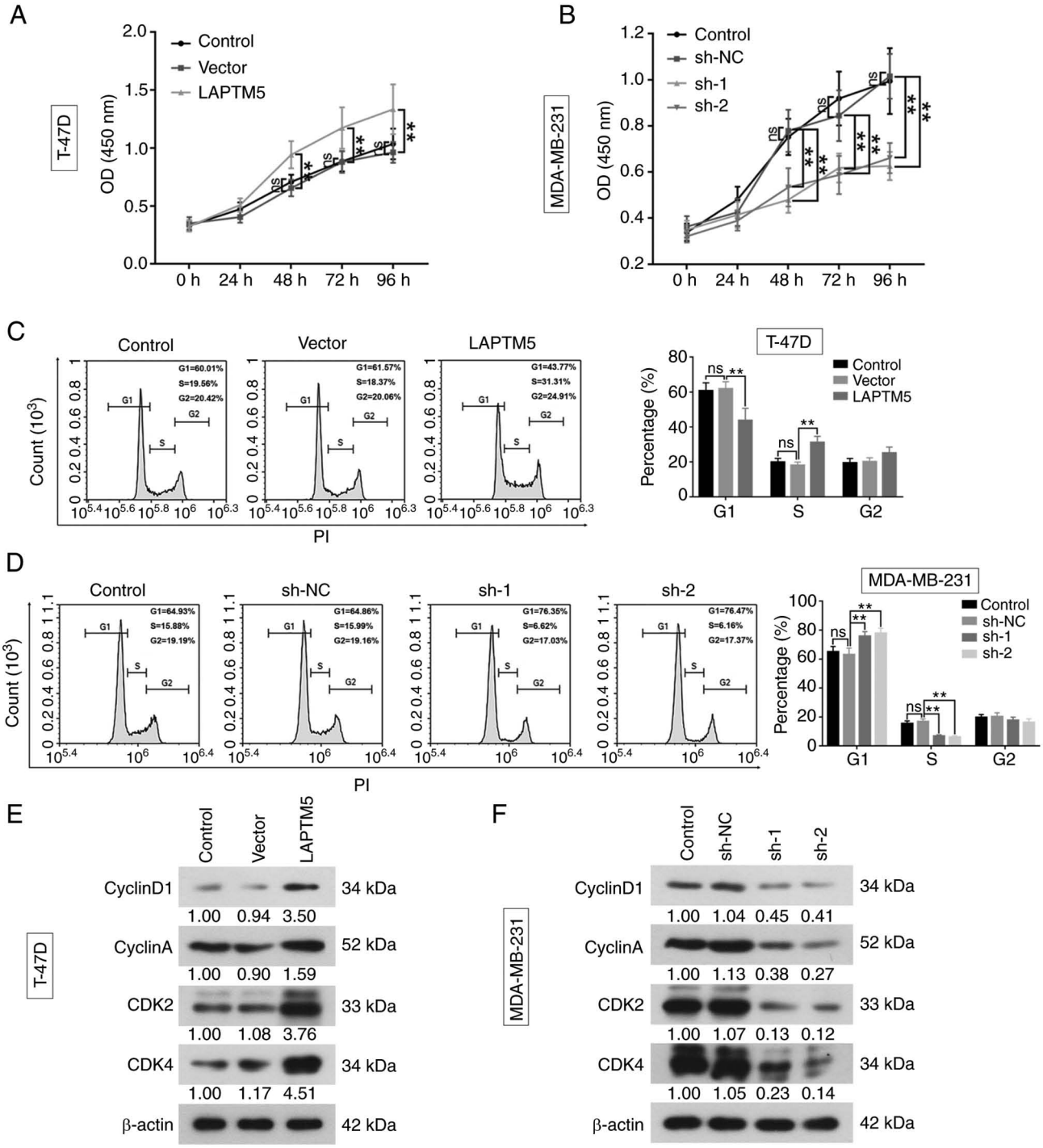

Figure 2. LAPTM5 promotes cell proliferation of breast cancer. (A and B) Cell Counting Kit-8 was used to evaluate cell proliferation of the two breast cancer cell lines at 0, 24, 48, 72 and 96 h. (C and D) The effects of LAPTM5 upregulation or downregulation on cell cycle were detected by flow cytometry. The percentage of cells at different stages of cell cycles was statistically analyzed. (E and F) The protein expression of CyclinD1, CyclinA, CDK2 and CDK4 was examined by western blot analysis. β-actin served as loading control. Data originated from three independent experiments and are presented as the mean ± SD. **P<0.01. LAPTM5, lysosomal protein transmembrane 5; ns, not significant; sh-, short hairpin; NC, negative control.

These results indicated that LAPTM5 promoted the process of cell migration, invasion and EMT.

LAPTM5 regulates the proliferation and migration of breast cancer cells by activation of the Wnt/β-catenin signaling pathway. To explore the mechanism of LAPTM5 in breast cancer, activated β-catenin expression was detected by western blotting. The nuclear β-catenin was upregulated by LAPTM5 overexpression and downregulated by silencing of LAPTM5 (Fig. 4A). Total β-catenin protein level was consistent with that in the nucleus. IF displayed that β-catenin expression was obviously increased in the nucleus when LAPTM5 was overexpressed, while, when LAPTM5 was downregulated, the level of β-catenin in the nucleus was decreased (Fig. 4B). Additionally, the mRNA and protein levels of β-catenin were successfully reduced by si-β-catenin in the T-47D cells (si-NC

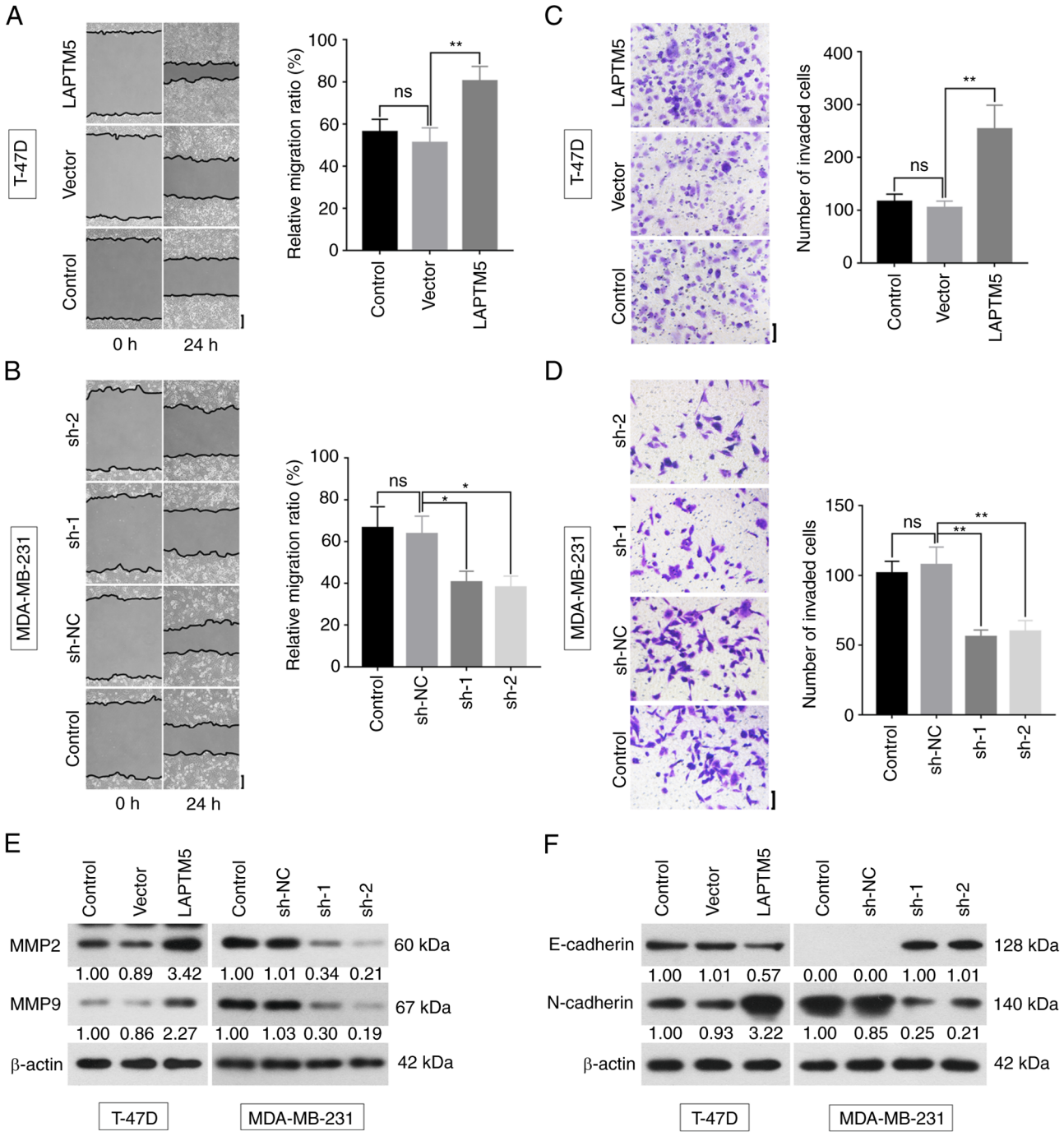

Figure 3. LAPTM5 promotes migration and invasion of breast cancer. (A and B) Cell metastatic ability was evaluated by wound healing assay at 0 and 24 h. The relative migration ratio was statistically analyzed. Scale bar, 200 μm. (C and D) Cell invasive ability was detected by Transwell assay. Number of invasive cells was statistically analyzed. Scale bar, 100 μm. (E and F) Protein expression of MMP2, MMP9, E-cadherin, and N-cadherin was examined by western blotting. Data originated from three independent experiments and are presented as the mean ± SD. *P<0.05 and **P<0.01. LAPTM5, lysosomal protein transmembrane 5; MMP, matrix metallopeptidase; ns, not significant; sh-, short hairpin; NC, negative control.

vs. si-β-catenin, 1.0140±0.0864 vs. 0.3042±0.0384, P<0.01, Fig. 4C). Furthermore, the results of CCK-8 assay indicated that si-β-catenin inhibited LAPTM5-induced cell proliferation (OE-LAPTM5 + si-NC vs. OE-LAPTM5 + si-β-catenin, 1.0730±0.1675 vs. 0.7153±0.0670, P<0.05, Fig. 4D). Wound healing assay demonstrated that downregulation of β-catenin suppressed the migration of LAPTM5-overexpressed breast cancer cells (OE-LAPTM5 + si-NC vs. OE-LAPTM5 + si-β-catenin, 79.2±6.8 vs. 57.7±6.4, P<0.05, Fig. 4E). The results of Transwell assay showed the same effects of β-catenin on cell invasion (OE-LAPTM5 + si-NC vs. OE-LAPTM5 + si-β-catenin, 255.9±33.6 vs. 125.7±13.7, P<0.01, Fig. 4E). Collectively, it was revealed that LAPTM5 promoted the cell malignant phenotypes of breast cancer through activating the Wnt/β-catenin signaling pathway.

LAPTM5 promotes breast cancer tumorigenesis in vivo. Based on the *in vitro* findings, the effects of LAPTM5 on

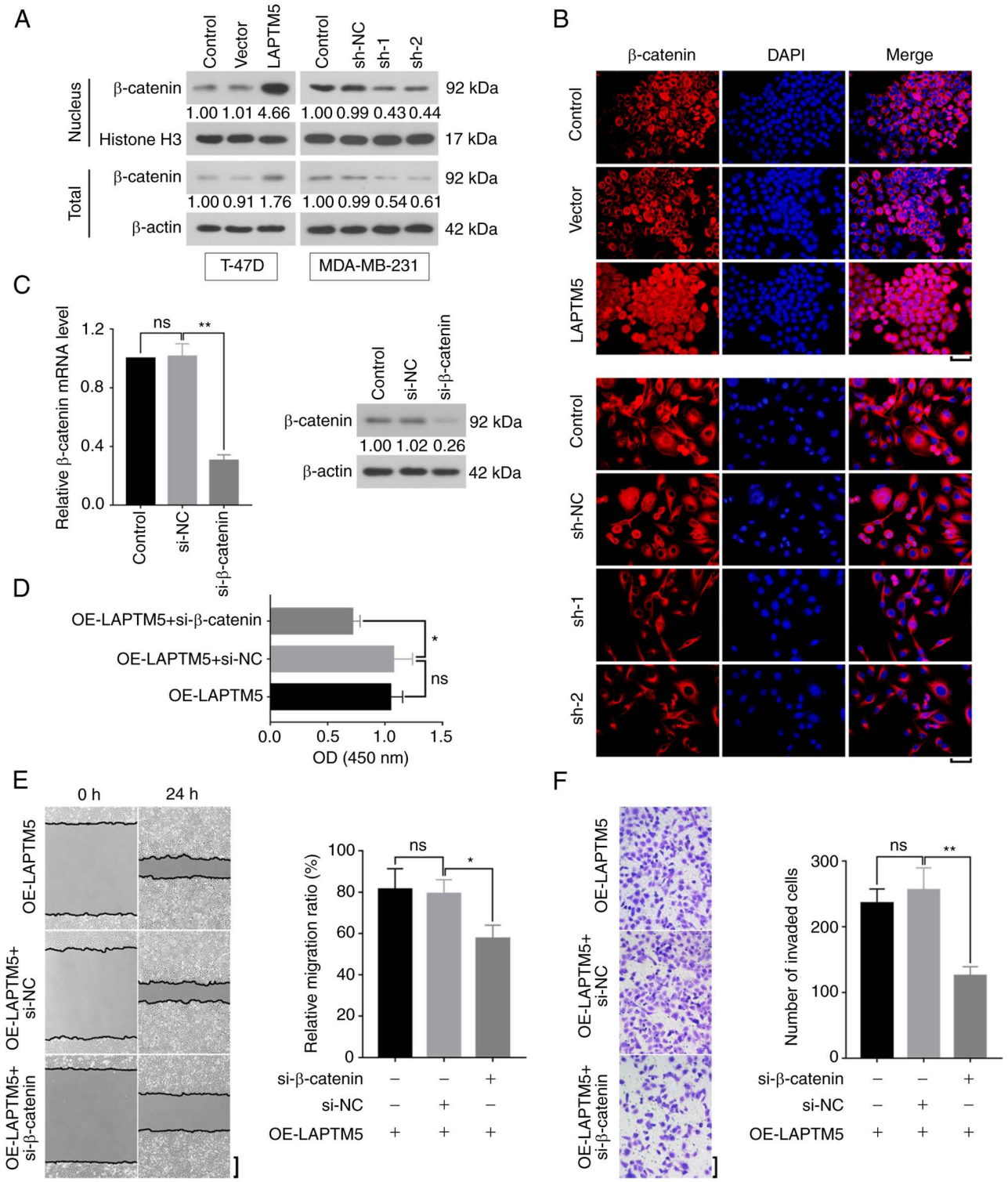

Figure 4. β-catenin mediates breast cancer development induced by LAPTM5. (A) Nuclear and total protein expression of β-catenin were detected by western blotting. Histone H3 was used as a loading control for the nucleoplasm protein. β-actin was used as a loading control for the total protein. (B) The location and activation of β-catenin was revealed by immunofluorescence. Scale bar, 50 μm. (C) The inhibition efficiency of β-catenin in the T-47D cells was detected by reverse transcription-quantitative PCR and western blotting. (D) Cell proliferation affected by overexpressed LAPTM5 and si-β-catenin was evaluated by Cell Counting Kit-8 assay. (E) The effect of si-β-catenin on LAPTM5 induced cell migration was revealed by wound healing assay. The relative migration ratio was statistically analyzed. Scale bar, 200 μm. (F) The effect of si-β-catenin on LAPTM5 induced cell invasion was detected by Transwell assay. Invasive cell number was statistically analyzed. Scale bar, 100 μm. Data originated from three independent experiments and are presented as the mean ± SD. *P<0.05 and **P<0.01. LAPTM5, lysosomal protein transmembrane 5; si-, small interfering; OE, overexpressing; ns, not significant; NC, negative control.

breast cancer were further investigated *in vivo*. After injection of T-47D cells to mice, tumor volume was significantly increased by LAPTM5 overexpression at day 18 (Vector vs. LAPTM5, 120.7±22.6 vs. 259.6±80.0, P<0.01), day 21 (Vector vs. LAPTM5, 163.8±28.7 vs. 329.1±106.0, P<0.01), day 24 (Vector vs. LAPTM5, 205.1±36.0 vs. 390.2±130.8,

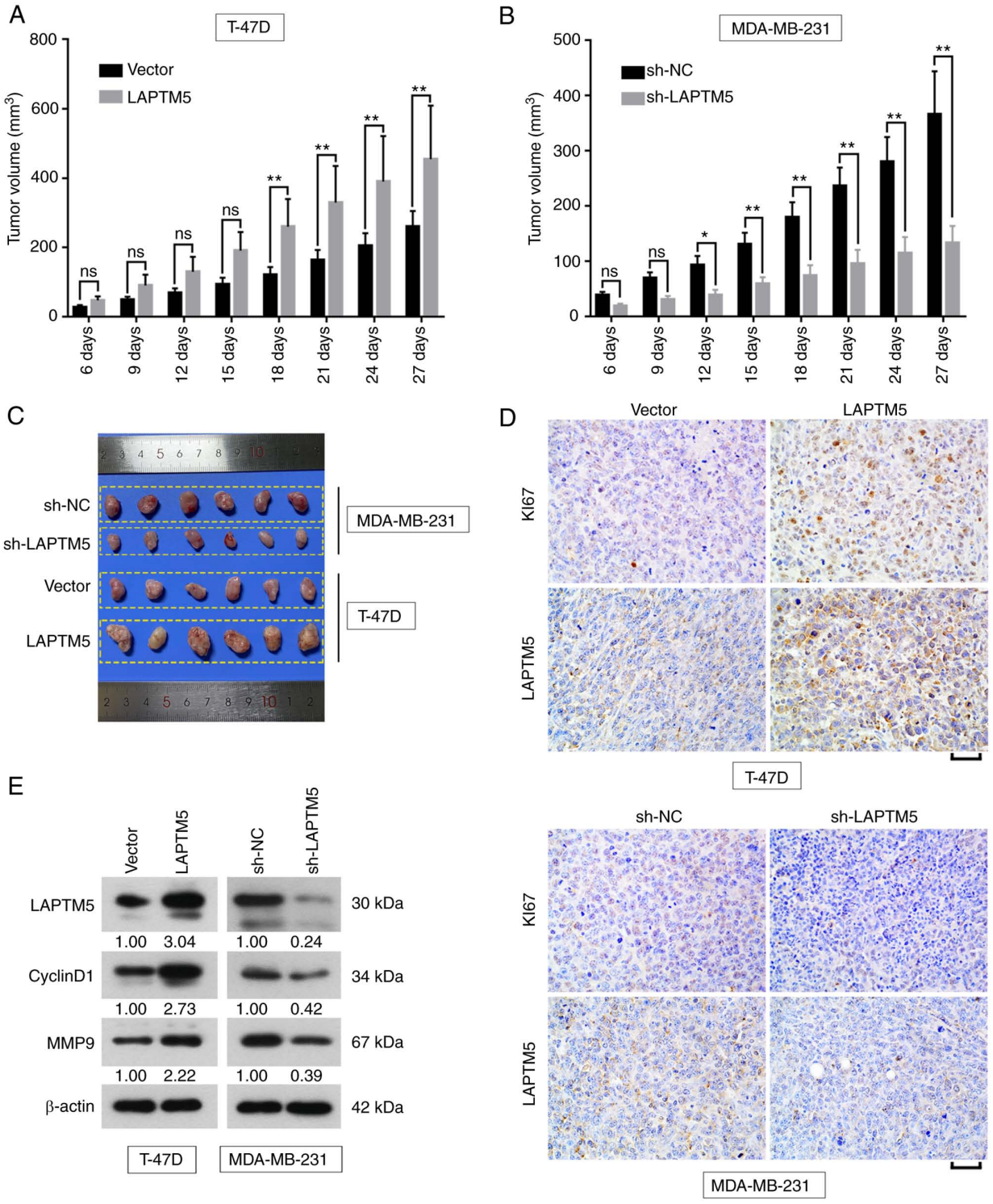

Figure 5. LAPTM5 promotes tumorigenesis of breast cancer *in vivo*. (A and B) Tumor volume of xenografts in mice injected with LAPTM5-overexcpressed T-47D or sh-LAPTM5 MDA-MB-231 was measured every 3 days until day 27. (C) Images of xenografts cultured for 27 days. (D) The expression of KI67 and LAPTM5 in xenografts was detected by immunohistochemistry. Scale bar, 50 μm. (E) Protein expression of LAPTM5, CyclinD1 and MMP9 in xenografts was evaluated by western blot analysis. Data originated from three independent experiments and are presented as the mean ± SD. *P<0.05 and **P<0.01. LAPTM5, lysosomal protein transmembrane 5; MMP, matrix metallopeptidase; ns, not significant; sh-, short hairpin; NC, negative control.

P<0.01) and day 27 (Vector vs. LAPTM5, 260.0±44.8 vs. 454.7±154.0, P<0.01, Fig. 5A). When LAPTM5 was knocked down *in vivo*, the size of xenograft was reduced at day 12 (sh-NC vs. sh-LAPTM5, 92.9±16.5 vs. 38.8±9.1, P<0.05), day 15 (sh-NC vs. sh-LAPTM5, 130.5±20.8 vs. 59.0±11.9, P<0.01), day 18 (sh-NC vs. sh-LAPTM5, 179.5±27.0 vs. 73.7±19.1, P<0.01), day 21 (sh-NC vs. sh-LAPTM5, 236.5±33.2 vs. 95.4±25.0, P<0.01), day 24 (sh-NC vs. sh-LAPTM5, 280.5±44.3 vs. 114.6±29.0, P<0.01) and day 27 (sh-NC vs. sh-LAPTM5, 366.1±78.0 vs. 133.1±30.8, P<0.01, Fig. 5B). The image of tumors at day 27 was presented in Fig. 5C. Furthermore, IHC results exhibited that KI67 was

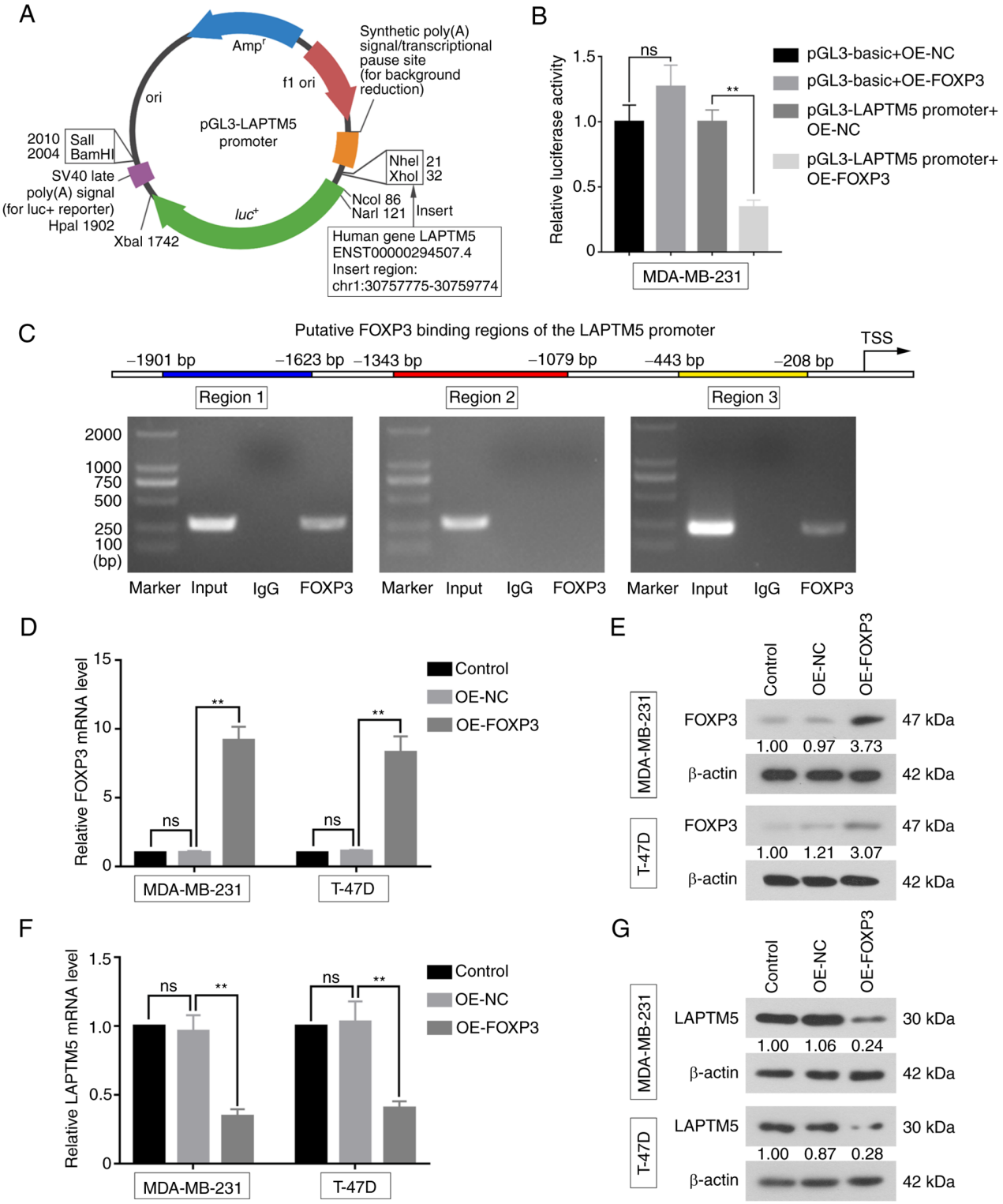

Figure 6. FOXP3 as a transcription suppressor binds to the promoter of LAPTM5. (A) The reporter plasmid of the pGL3-LAPTM5 promoter. (B) The relative luciferase activity in MDA-MB-231 treated by four groups revealed the regulation of FOXP3 on LAPTM5. (C) Chromatin immunoprecipitation was used to explore the binding sites of FOXP3 targeting LAPTM5 promoter. TSS in the image was the transcription starting point of LAPTM5. (D and E) The overexpression efficiency of FOXP3 on mRNA and protein expression level were evaluated by RT-qPCR and western blot analysis. (F and G) The mRNA and protein expression of LAPTM5 affected by FOXP3 overexpression were evaluated by RT-qPCR and western blotting. Data originated from three independent experiments and are presented as the mean ± SD. **P<0.01. FOXP3, forkhead box protein 3; LAPTM5, lysosomal protein transmembrane 5; TSS, transcription start site; RT-qPCR, reverse transcription-quantitative PCR; OE, overexpressing; ns, not significant; NC, negative control.

remarkably increased by LAPTM5 overexpression in the tumor, while, the expression of KI67 was decreased by suppressing LAPTM5 (Fig. 5D). The protein expression of CyclinD1 and MMP9 was obviously enhanced by upregulation of LAPTM5, and was reduced by the downregulation of LAPTM5 (Fig. 5E). The aforementioned findings illustrated

that LAPTM5 functioned as a promoter of tumor growth *in vivo*.

FOXP3 binds to the LAPTM5 promoter region and suppresses its expression. The present study investigated whether LAPTM5 was regulated by FOXP3 via the dual-luciferase reporter assay. The LAPTM5 promoter region was first inserted into the pGL3-basic luciferase reporter vector (Fig. 6A). Compared with the OE-NC group, relative luciferase activity of MDA-MB-231 cells co-transfected with OE-FOXP3 and pGL3-LAPTM5 promoter was significantly decreased (pGL3-LAPTM5 promoter + OE-NC vs. pGL3-LAPTM5 promoter + OE-FOXP3, 1.0000±0.0900 vs. 0.3433±0.0551, P<0.01), indicating that FOXP3 could bind to the LAPTM5 promoter (Fig. 6B). Additionally, ChIP assays were performed to evaluate whether FOXP3 directly binds to the LAPTM5 promoter. The primers on region 1 and region 3 of the LAPTM5 promoter generated positive products (Fig. 6C), suggesting that FOXP3 could directly bind to these two regions of the LAPTM5 promoter. Furthermore, the mRNA expression of FOXP3 was significantly upregulated in MDA-MB-231 (OE-NC vs. OE-FOXP3, 1.0350±0.0905 vs. 9.1760±0.9873, P<0.01) and T-47D cells (OE-NC vs. OE-FOXP3, 1.1220±0.0901 vs. 8.3090±1.1550, P<0.01), and protein expression displayed the same trends (Fig. 6D and E). As expected, the relative mRNA expression of LAPTM5 was downregulated with FOXP3 overexpression in MDA-MB-231 (OE-NC vs. OE-FOXP3, 0.9627±0.1170 vs. 0.3445±0.0506, P<0.01) and T-47D cells (OE-NC vs. OE-FOXP3, 1.0300±0.1510 vs. 0.4045±0.0485, P<0.01, Fig. 6F). Meanwhile, LAPTM5 protein expression was suppressed in the FOXP3-overexpressed cells (Fig. 6G). These findings demonstrated that FOXP3 could bind to the LAPTM5 promoter and act as a transcriptional suppressor of LAPTM5 in breast cancer cells.

Discussion

The relapse and metastasis of breast cancer spread to distant sites remain the leading causes of morbidity and mortality associated with this disease (9). To optimize the diagnostic methods and reduce the mortality of patients with breast cancer, it is urgent to identify molecular targets that participate in cancer cell metastasis and invasion. The present study found that the expression of LAPTM5 was significantly higher in breast cancer tissues than that in para cancer tissues. The results are consistent with those from previous studies on human tumors, such as bladder cancer (BCa). Microarray analysis was used to determine that LAPTM5 was upregulated in BCa tissues at both mRNA and protein levels (12). Besides, LAPTM5 was abnormally highly expressed in TGCT, and the prognosis of the LAPTM5 high-expression group was significantly worse than that of the low-expression group (11). In addition, LAPTM5 was highly expressed in CCRCC, which was significantly associated with the survival prognosis of CCRCC (13). In the present study, the association between clinical indicators and LAPTM5 expression was analyzed. It displayed that LAPTM5 was significantly positive-associated with SBR grading and NPI, which were the major tumor grading methods of breast cancer in clinical judgement. High expression of LAPTM5 was also indicated to associate with worse overall survival. Based on these results, the status of LAPTM5 expression may be a potential indicator for tumor stage of breast cancer, which was worth evaluating in clinical applications. Moreover, a previous study found that LAPTM 4 beta (LAPTM4B), which belongs to the same lysosomal membrane protein as LAPTM5, was upregulated in breast cancer, and its high expression was positively related to TNM stage and lymph node metastasis (33). Recently, Meng *et al* (34) found that LAPTM5 regulated the development and spinal metastasis of ER-positive breast cancer through the glutamine-dependent mTOR signaling, while the present study demonstrated that LAPTM5, which is affected by the transcription factor FOXP3, could contribute to the tumor progression of breast cancer via the Wnt/β-catenin signaling pathway (Fig. 7).

The experiments *in vitro* and *in vivo* identified that the upregulation of LAPTM5 increased the number of cells in S phase and enhanced the expression of proliferation marker genes. CyclinD1 facilitates the transition from G1 to the S phase of the cell cycle by activating CDK4 or CDK6 (35). Meanwhile, CyclinA and CDK2 drive S phase progression and DNA synthesis (36). When LAPTM5 was overexpressed, these proteins expressed higher levels, and cells were enriched in the S phase, which is the main stage of DNA synthesis. By contrast, downregulation of LAPTM5 suppressed the expression of CyclinD1, CyclinA, CDK2 and CDK4, and decreased the number of S phase cells. Overall, these results suggested that LAPTM5 promoted cell proliferation. Moreover, it was found that MMP2, MMP9 and N-cadherin were increased with upregulation of LAPTM5, while they were decreased when LAPTM5 was downregulated. The expression of E-cadherin led to opposite expression patterns of the aforementioned proteins, which are closely associated with cell invasion. Based on these results, LAPTM5 was verified to promote EMT progress. Importantly, β-catenin was upregulated with the overexpression of LAPTM5, while downregulation of LAPTM5 produced the opposite effects. The Wnt/β-catenin signaling pathway plays an important role in cell development and differentiation, and is closely associated with different types of diseases and human cancer (37). β-catenin initiates the downstream transcription of genes such as CyclinD1 and MMPs (38), and is an essential binding partner of various cadherins, such as E-cadherin in adhesion junctions (39). Furthermore, the Wnt/β-catenin signaling pathway plays a crucial role in regulating EMT (40-42). All the aforementioned evidence demonstrated that LAPTM5 affected the development of breast cancer through activating the Wnt/β-catenin signaling pathway.

Numerous studies have revealed that transcription factors participate in cancer pathogenesis through the activation or inactivation of different genes. As a transcription factor, FOXP3 is well-known to play a regulatory role in human cancer. Concerning the mechanisms by which FOXP3 expression inhibits cancer metastasis, previous studies have been published in different types of tumors (16,43,44). Such as in ovarian cancer, cell metastasis and invasion were suppressed by FOXP3, and the expression of MMP-2 was reduced at the same time. Furthermore, previous studies indicated that FOXP3 could block the initiation of tumors, such as prostate cancer (45), as well as breast cancer (17,46). FOXP3 was identified to suppress the migration, proliferation and invasion

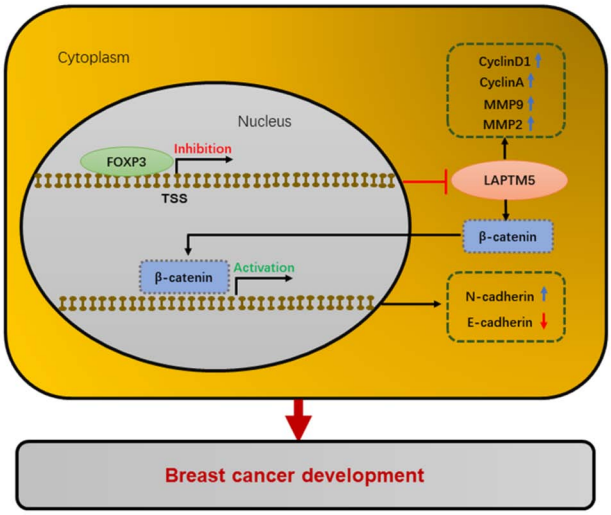

Figure 7. Underlying mechanism of LAPTM5 in breast cancer. LAPTM5 suppressed by FOXP3 promotes cell proliferation, migration, invasion, and epithelial-mesenchymal transition in breast cancer by activating the Wnt/β-catenin pathway. LAPTM5, lysosomal protein transmembrane 5; FOXP3, forkhead box protein 3.

of tumor cells (47). In addition, FOXP3 has been reported to inhibit breast cancer tumorigenesis, metastasis and invasion by regulating the expression of C-X-C Motif Chemokine Receptor 4, SATB homeobox 1, and S-phase kinase associated protein 2 (46,48,49). The association between FOXP3 and LAPTM5 was predicted, and certain binding sites were found in the LAPTM5 promoter region. Western blot results showed that the expression of LAPTM5 was negatively regulated by FOXP3. In addition, luciferase reporter and ChIP assays indicated FOXP3 surely interacted with LAPTM5. FOXP3 was found to affect the expression of LAPTM5 by binding its promoter region. Therefore, the results of the present study suggested that FOXP3 may inhibit development of breast cancer through regulating the expression of LAPTM5 and the Wnt/β-catenin signaling pathway.

It is well known that estrogen and progesterone are crucial factors involved in breast cancer (50,51). Hormonotherapy is an effective treatment therapy for patients with hormone-positive breast cancer. Among all subtypes of breast cancer, triple-negative breast cancer is a specific subtype, which has high invasiveness and poor prognosis (52,53). LAPTM5 was expressed at higher levels in ER- or PR-breast cancer samples, which indicated that breast cancer patients with high LAPTM5 level may experience greater treatment difficulties, and that the expression of LAPTM5 may be restricted by hormones. The present study did not explore the role of LAPTM5 in triple negative breast cancer cell lines, which is a limitation. Therefore, it is planned to investigate the mechanism by which hormones affect the expression of LAPTM5, and how to improve clinical hormone therapy based on this mechanism.

Experimental cancers may bring pain or suffering to tumor-bearing animals. Therefore, the associations of experimental animals suggest implementing humane endpoints in cancer research. The present study was carried out in accordance with the regulations of Chinese Association for Laboratory Animal Science-Laboratory animal-Guidelines for euthanasia (2017), which specified the humanitarian endpoint on subcutaneous xenograft tumors: i) Tumor exceeds 10% of the host's original body weight; ii) Weight loss reached 20-25% of the original body weight. In the present study, the maximum weight loss rate of tumor-bearing mice was 4.79%, and the maximum tumor volume was 506.47 mm^3. The tumor weight was not measured in the present study, but it was estimated via weighing the tumors with similar volume in other studies (experiment in progress; Chi *et al*, unpublished data), and the results showed that tumor volume at 500±5 mm^3 weighs 0.5±0.05 g, which is ~2-3% of the host's body weight. Thus, the mice in the present study did not reach the humanitarian endpoint specified in the aforementioned literature. In addition, inquiries regarding suggestions on the humane endpoints were also addressed to certain international ethical organizations, including UK Co-ordinating Committee on Cancer Research (UKCCCR Guidelines for the Welfare of Animals in Experimental Neoplasia, 1997) and National Institutes of Health (Institutional Animal Care and Use Committee Guidebook, 2002). It was stipulated that when tumor exceeds 10% of normal body weight or results in rapid body weight loss of 20%, the humanitarian endpoint for execution of experimental mice is reached. Therefore, it can be clearly observed that the experimental mice in the present study, whether at home or abroad, were far from meeting the requirement of humane endpoint. Certainly, the authors also agree that it is very important to weigh the tumors, and this issue shall be addressed in the future study.

In addition, the goal of the authors is to investigate the pathogenesis of breast cancer and investigate for potential therapeutic molecules. The LAPTM5 was initially displayed as CLAST6, which was found from high-throughput sequencing results in the authors' research group (Chi *et al*, unpublished data). The roles of the other abnormally expressed genes in breast cancer shall be investigated in further research.

In summary, the present study provided evidence that LAPTM5 may exert its biological functions of enhancing cell proliferation, migration, invasion and EMT of breast cancer cells via the activation of the Wnt/β-catenin signaling pathway, and demonstrated that LAPTM5 was negatively regulated by the transcription factor FOXP3.

Acknowledgements

Not applicable.

Funding

No funding was received.

Availability of data and materials

The datasets used and/or analyzed during the current study are available from the corresponding author on reasonable request.

Authors' contributions

SH performed the main experiments and drafted the manuscript. XJ analyzed the data and prepared the figures. TH

participated in cell culture and infection. FC designed the research and revised the manuscript. SH, XJ, TH and FC confirm the authenticity of all the raw data. All authors read and approved the final version of the manuscript.

Ethics approval and consent to participate

Human studies were performed in accordance with the Declaration of Helsinki and were approved (approval no. 2019PS339K) by the ethics committee of Shengjing Hospital of China Medical University. Written informed consent was provided by all patients. The animal experiment protocol complied with the international guidelines and was approved (approval no. 2019PS339K) by the animal ethics committee of Shengjing Hospital of China Medical University (Shenyang, China).

Patient consent for publication

Not applicable.

Competing interests

The authors declare that they have no competing interests.

References

1. Jalkh N, Nassar-Slaba J, Chouery E, Salem N, Uhrchammer N, Golmard L, Stoppa-Lyonnet D, Bignon YJ and Mégarbané A: Prevalance of BRCA1 and BRCA2 mutations in familial breast cancer patients in Lebanon. Hered Cancer Clin Pract 10: 7, 2012.
2. Coughlin SS and Ekwueme DU: Breast cancer as a global health concern. Cancer Epidemiol 33: 315-318, 2009.
3. Benson JR, Jatoi I, Keisch M, Esteva FJ, Makris A and Jordan VC: Early breast cancer. Lancet 373: 1463-1479, 2009.
4. Lv W, Chen N, Lin Y, Ma H, Ruan Y, Li Z, Li X, Pan X and Tian X: Macrophage migration inhibitory factor promotes breast cancer metastasis via activation of HMGB1/TLR4/NF kappa B axis. Cancer Lett 375: 245-255, 2016.
5. Ghislain I, Zikos E, Coens C, Quinten C, Balta V, Tryfonidis K, Piccart M, Zardavas D, Nagele E, Bjelic-Radisic V, *et al*: Health-related quality of life in locally advanced and metastatic breast cancer: Methodological and clinical issues in randomised controlled trials. Lancet Oncol 17: e294-e304, 2016.
6. Luo J, Yao JF, Deng XF, Zheng XD, Jia M, Wang YQ, Huang Y and Zhu JH: 14, 15-EET induces breast cancer cell EMT and cisplatin resistance by up-regulating integrin αvβ3 and activating FAK/PI3K/AKT signaling. J Exp Clin Cancer Res 37: 23, 2018.
7. Sun L, Yao Y, Liu B, Lin Z, Lin L, Yang M, Zhang W, Chen W, Pan C, Liu Q, *et al*: MiR-200b and miR-15b regulate chemotherapy-induced epithelial-mesenchymal transition in human tongue cancer cells by targeting BMI1. Oncogene 31: 432-445, 2012.
8. Mani SA, Guo W, Liao MJ, Eaton EN, Ayyanan A, Zhou AY, Brooks M, Reinhard F, Zhang CC, Shipitsin M, *et al*: The epithelial-mesenchymal transition generates cells with properties of stem cells. Cell 133: 704-715, 2008.
9. DiMeo TA, Anderson K, Phadke P, Fan C, Perou CM, Naber S and Kuperwasser C: A novel lung metastasis signature links Wnt signaling with cancer cell self-renewal and epithelial-mesenchymal transition in basal-like breast cancer. Cancer Res 69: 5364-5373, 2009.
10. Nuylan M, Kawano T, Inazawa J and Inoue J: Down-regulation of LAPTM5 in human cancer cells. Oncotarget 7: 28320-28328, 2016.
11. Li X, Su Y, Zhang J, Zhu Y, Xu Y and Wu G: LAPTM5 plays a Key role in the diagnosis and prognosis of testicular germ cell tumors. Int J Genomics 2021: 8816456, 2021.
12. Chen L, Wang G, Luo Y, Wang Y, Xie C, Jiang W, Xiao Y, Qian G and Wang X: Downregulation of LAPTM5 suppresses cell proliferation and viability inducing cell cycle arrest at G0/G1 phase of bladder cancer cells. Int J Oncol 50: 263-271, 2017.
13. Sui Y, Lu K and Fu L: Prediction and analysis of novel key genes ITGAX, LAPTM5, SERPINE1 in clear cell renal cell carcinoma through bioinformatics analysis. PeerJ 9: e11272, 2021.
14. Brunkow ME, Jeffery EW, Hjerrild KA, Paeper B, Clark LB, Yasayko SA, Wilkinson JE, Galas D, Ziegler SF and Ramsdell F: Disruption of a new forkhead/winged-helix protein, scurfin, results in the fatal lymphoproliferative disorder of the scurfy mouse. Nat Genet 27: 68-73, 2001.
15. Szylberg Ł, Karbownik D and Marszałek A: The role of FOXP3 in human cancers. Anticancer Res 36: 3789-3794, 2016.
16. Zhang C, Xu Y, Hao Q, Wang S, Li H, Li J, Gao Y, Li M, Li W, Xue X, *et al*: FOXP3 suppresses breast cancer metastasis through downregulation of CD44. Int J Cancer 137: 1279-1290, 2015.
17. Zuo T, Wang L, Morrison C, Chang X, Zhang H, Li W, Liu Y, Wang Y, Liu X, Chan MWY, *et al*: FOXP3 is an X-linked breast cancer suppressor gene and an important repressor of the HER-2/ErbB2 oncogene. Cell 129: 1275-1286, 2007.
18. Douglass S, Ali S, Meeson AP, Browell D and Kirby JA: The role of FOXP3 in the development and metastatic spread of breast cancer. Cancer Metastasis Rev 31: 843-854, 2012.
19. Ladoire S, Mignot G, Dalban C, Chevriaux A, Arnould L, Rébé C, Apetoh L, Boidot R, Penault-Llorca F, Fumoleau P, *et al*: FOXP3 expression in cancer cells and anthracyclines efficacy in patients with primary breast cancer treated with adjuvant chemotherapy in the phase III UNICANCER-PACS 01 trial. Ann Oncol 23: 2552-2561, 2012.
20. Bahrami A, Hasanzadeh M, ShahidSales S, Yousefi Z, Kadkhodayan S, Farazestanian M, Joudi Mashhad M, Gharib M, Mahdi Hassanian S and Avan A: Clinical significance and prognosis value of Wnt signaling pathway in cervical cancer. J Cell Biochem 118: 3028-3033, 2017.
21. Liu J and Wang Y: Long non-coding RNA KCNQ1OT1 facilitates the progression of cervical cancer and tumor growth through modulating miR-296-5p/HYOU1 axis. Bioengineered 12: 8753-8767, 2021.
22. Clevers H and Nusse R: Wnt/β-catenin signaling and disease. Cell 149: 1192-1205, 2012.
23. Kypta RM and Waxman J: Wnt/β-catenin signalling in prostate cancer. Nat Rev Urol 9: 418-428, 2012.
24. Wang Z, Li B, Zhou L, Yu S, Su Z, Song J, Sun Q, Sha O, Wang X, Jiang W, *et al*: Prodigiosin inhibits Wnt/β-catenin signaling and exerts anticancer activity in breast cancer cells. Proc Natl Acad Sci USA 113: 13150-13155, 2016.
25. Li Y, Jin K, van Pelt GW, van Dam H, Yu X, Mesker WE, Ten Dijke P, Zhou F and Zhang L: c-Myb enhances breast cancer invasion and metastasis through the Wnt/β-catenin/Axin2 pathway. Cancer Res 76: 3364-3375, 2016.
26. Dey N, Barwick BG, Moreno CS, Ordanic-Kodani M, Chen Z, Oprea-Ilies G, Tang W, Catzavelos C, Kerstann KF, Sledge GW Jr, *et al*: Wnt signaling in triple negative breast cancer is associated with metastasis. BMC Cancer 13: 537, 2013.
27. Jézéquel P, Gouraud W, Ben Azzouz F, Guérin-Charbonnel C, Juin PP, Lasla H and Campone M: bc-GenExMiner 4.5: New mining module computes breast cancer differential gene expression analyses. Database (Oxford) 2021: baab007, 2021.
28. Lánczky A and Győrffy B: Web-based survival analysis tool tailored for medical research (KMplot): Development and implementation. J Med Internet Res 23: e27633, 2021.
29. Livak KJ and Schmittgen TD: Analysis of relative gene expression data using real-time quantitative PCR and the 2(-Delta Delta C(T)) method. Methods 25: 402-408, 2001.
30. Amat S, Penault-Llorca F, Cure H, Le Bouedëc G, Achard JL, Van Praagh I, Feillel V, Mouret-Reynier MA, Dauplat J and Chollet P: Scarff-bloom-richardson (SBR) grading: A pleiotropic marker of chemosensitivity in invasive ductal breast carcinomas treated by neoadjuvant chemotherapy. Int J Oncol 20: 791-796, 2002.
31. Corso G, Figueiredo J, De Angelis SP, Corso F, Girardi A, Pereira J, Seruca R, Bonanni B, Carneiro P, Pravettoni G, *et al*: E-cadherin deregulation in breast cancer. J Cell Mol Med 24: 5930-5936, 2020.
32. Thiery JP, Acloque H, Huang RYJ and Nieto MA: Epithelial-mesenchymal transitions in development and disease. Cell 139: 871-890, 2009.
33. Xiao M, Jia S, Wang H, Wang J, Huang Y and Li Z: Overexpression of LAPTM4B: An independent prognostic marker in breast cancer. J Cancer Res Clin Oncol 139: 661-667, 2013.

34. Meng Q, Zhou L, Liang H, Hu A, Zhou H, Zhou J, Zhou X, Lin H, Li X, Jiang L and Dong J: Spine-specific downregulation of LAPTM5 expression promotes the progression and spinal metastasis of estrogen receptor-positive breast cancer by activating glutamine-dependent mTOR signaling. Int J Oncol 60: 47, 2022.
35. Hosooka T and Ogawa W: A novel role for the cell cycle regulatory complex cyclin D1-CDK4 in gluconeogenesis. J Diabetes Investig 7: 27-28, 2016.
36. Malumbres M and Barbacid M: Mammalian cyclin-dependent kinases. Trends Biochem Sci 30: 630-641, 2005.
37. Nishisho I, Nakamura Y, Miyoshi Y, Miki Y, Ando H, Horii A, Koyama K, Utsunomiya J, Baba S and Hedge P: Mutations of chromosome 5q21 genes in FAP and colorectal cancer patients. Science 253: 665-669, 1991.
38. Yang M, Wang M, Li X, Xie Y, Xia X, Tian J, Zhang K and Tang A: Wnt signaling in cervical cancer? J Cancer 9: 1277-1286, 2018.
39. Peifer M, McCrea PD, Green KJ, Wieschaus E and Gumbiner BM: The vertebrate adhesive junction proteins beta-catenin and plakoglobin and the Drosophila segment polarity gene armadillo form a multigene family with similar properties. J Cell Biol 118: 681-691, 1992.
40. Gao Y, Chen Z, Wang R, Tan X, Huang C, Chen G and Chen Z: LXRα promotes the differentiation of human gastric cancer cells through inactivation of Wnt/β-catenin signaling. J Cancer 10: 156-167, 2019.
41. Yeh Y, Guo Q, Connelly Z, Cheng S, Yang S, Prieto-Dominguez N and Yu X: Wnt/beta-catenin signaling and prostate cancer therapy resistance. Adv Exp Med Biol 1210: 351-378, 2019.
42. Peng N, Zhang Z, Wang Y, Yang M, Fan J, Wang Q, Deng L, Chen D, Cai Y, Li Q, *et al*: Down-regulated LINC00115 inhibits prostate cancer cell proliferation and invasion via targeting miR-212-5p/FZD5/Wnt/β-catenin axis. J Cell Mol Med 25: 10627-10637, 2021.
43. Gong Z, Jia H, Yu J, Liu Y, Ren J, Yang S, Hu B, Liu L, Lai PBS and Chen GG: Nuclear FOXP3 inhibits tumor growth and induced apoptosis in hepatocellular carcinoma by targeting c-Myc. Oncogenesis 9: 97, 2020.
44. Liu C, Han J, Li X, Huang T, Gao Y, Wang B, Zhang K, Wang S, Zhang W, Li W, *et al*: FOXP3 inhibits the metastasis of breast cancer by downregulating the expression of MTA1. Front Oncol 11: 656190, 2021.
45. Wang L, Liu R, Li W, Chen C, Katoh H, Chen GY, McNally B, Lin L, Zhou P, Zuo T, *et al*: Somatic single hits inactivate the X-linked tumor suppressor FOXP3 in the prostate. Cancer Cell 16: 336-346, 2009.
46. Zuo T, Liu R, Zhang H, Chang X, Liu Y, Wang L, Zheng P and Liu Y: FOXP3 is a novel transcriptional repressor for the breast cancer oncogene SKP2. J Clin Invest 117: 3765-3773, 2007.
47. Huang Z, Liu F, Wang W, Ouyang S, Sang T, Huang Z, Liao L and Wu J: Deregulation of circ_003912 contributes to pathogenesis of erosive oral lichen planus by via sponging microRNA-123, -647 and -31 and upregulating FOXP3. Mol Med 27: 132, 2021.
48. Douglass S, Meeson AP, Overbeck-Zubrzycka D, Brain JG, Bennett MR, Lamb CA, Lennard TW, Browell D, Ali S and Kirby JA: Breast cancer metastasis: Demonstration that FOXP3 regulates CXCR4 expression and the response to CXCL12. J Pathol 234: 74-85, 2014.
49. McInnes N, Sadlon TJ, Brown CY, Pederson S, Beyer M, Schultze JL, McColl S, Goodall GJ and Barry SC: FOXP3 and FOXP3-regulated microRNAs suppress SATB1 in breast cancer cells. Oncogene 31: 1045-1054, 2012.
50. Hilton HN, Clarke CL and Graham JD: Estrogen and progesterone signalling in the normal breast and its implications for cancer development. Mol Cell Endocrinol 466: 2-14, 2018.
51. Russo J and Russo IH: Development of the human breast. Maturitas 49: 2-15, 2004.
52. Yin L, Duan JJ, Bian XW and Yu SC: Triple-negative breast cancer molecular subtyping and treatment progress. Breast Cancer Res 22: 61, 2020.
53. Borri F and Granaglia A: Pathology of triple negative breast cancer. Semin Cancer Biol 72: 136-145, 2021.